An Acad Bras Cienc (2023) 95(1): e20220177 DOI 10.1590/0001-3765202320220177
Anais da Academia Brasileira de Ciências | *Annals of the Brazilian Academy of Sciences*
Printed ISSN 0001-3765 I Online ISSN 1678-2690
www.scielo.br/aabc | www.fb.com/aabcjournal

GEOSCIENCES

Monitoring river turbidity after a mine tailing dam failure using an empirical model derived from Sentinel-2 imagery

PEDRO L.B. CRIONI, ELIAS H. TERAMOTO & HUNG K. CHANG

Abstract: Sudden failure of a mine tailing dam occurred in the municipality of Brumadinho, Minas Gerais, Brazil, on January 25, 2019. Approximately 12 million cubic meters of mine tailings discharged into the Paraopeba River, producing strong environmental and societal impacts, mainly due to a massive increase in turbidity (occasionally exceeding 50,000 Nephelometric Turbidity Units [NTU] (CPRM 2019). Remote sensing is a well-established tool for quantifying spatial patterns of turbidity. However, a few empirical models have been developed to map turbidity in rivers impacted by mine tailings. Thus, this study aimed to develop an empirical model capable of producing turbidity estimates based on images from the Sentinel-2 satellite, using the Paraopeba River as the study area. We found that river turbidity was most strongly correlated with the sensor's near-infrared band (NIR) (band 8). Thus, we built an empirical single-band model using an exponential function with an (R^2 of 0.91) to characterize the spatial-temporal variation of turbidity based on satellite observations of NIR reflectance. Although the role of discharged tailings in the seasonal variation of turbidity is not well understood, the proposed model enabled the monitoring of turbidity variations in the Paraopeba River associated with seasonal resuspension or deposition of mine tailings. Our study shows the capability of single-band models to quantify seasonal variations in turbidity in rivers impacted by mine tailing pollution.

Key words: Mine tailings, Paraopeba river, Remote Sensing, Sentinel-2, turbidity, water quality.

INTRODUCTION

Turbidity is an optical parameter that is used to characterize water clarity, which is an important aspect of water quality (Davies-Colley & Smith 2001). This parameter is derived from measurements of the amount of stray light scattered as the incident light interacts with the material suspended in the water. Turbidity increases with the amount of material suspended in the water, consequently decreasing the intensity of scattered light (Davies-Colley & Smith 2001).

Anthropic increases in turbidity are known to negatively impact local aquatic ecology in various ways (e.g., Kirk 1985, Henley et al. 2000, Davies-Colley & Smith 2001, Bilotta & Brazier 2008). The most critical impact of increased turbidity on aquatic ecology is related to the rate of attenuation of solar radiation with depth, which can greatly decrease the euphotic (illuminated zone of aquatic ecosystems) depth of a body of water (Henley et al. 2000). Such decreases in euphotic depth have been linked to significant declines in local food chains, beginning at the primary trophic level (Kirk 1985, Henley et al. 2000, Bilotta & Brazier 2008). Moreover, the turbidity of drinking water should not exceed 5 NTU and would preferably remain

below 1 NTU (WHO 2017). This is because a high concentration of suspended solids in water results in a decrease in the potability of the water, rendering it unsuitable for consumption.

Turbidity varies broadly in response to the type, composition, size, and geometry of the suspended particles (Davies-Colley & Smith 2001). Because of the mix of natural and anthropic conditions across river basins, the range of river turbidity reported in different rivers can vary by several orders of magnitude (e.g., Huang et al. 1992, Wass et al. 1997, Göransson et al. 2013, Kuhn et al. 2019). Among the anthropic agents that increase turbidity, mining activity is recognized as one of the most important factors affecting surface waters worldwide (e.g., Thomas et al. 2003, Petticrew et al. 2015, Rudorff et al. 2018, Hamilton et al. 2020).

An example of the severe impacts of turbidity in a river caused by the influx of mine tailings occurred recently in the Brumadinho municipality, located in Minas Gerais State, southeastern Brazil. In January 2019, a mine tailings dam failed and released approximately 12 million cubic meters of tailings. A large proportion of the released tailings reached the Paraopeba River, an important regional river, causing serious environmental and societal damages (Polignano & Lemos 2020, Santos et al. 2021). The water supply to riverine communities that benefit from this water resource was directly affected (Polignano & Lemos 2020). Immediately after the dam failure, the water quality was monitored daily to assess the long-term effects of mine tailings on the river. The most critical impact observed was turbidity, which reached values above 50,000 NTU, which is 10,000 times greater than the standard limit for drinking water (WHO 2017).

As water turbidity can be considered an optical property, this parameter can be correlated with the spectral reflectance retrieved from satellite imagery (e.g., Caballero et al. 2019, Pereira et al. 2018, Kuhn et al. 2019). Several studies have quantitatively assessed river turbidity using remote sensing techniques (e.g., Wass et al. 1997, Petus et al. 2010, Pereira et al. 2018, Kuhn et al. 2019). The estimation of turbidity by remote sensing is based on the empirical association between the spectral reflectance measured via satellite imaging and turbidity values measured in the field. This approach can facilitate water quality management because these methods, allow continuous measurement of large regions (Caballero et al. 2019). Moreover, the acquisition of satellite imagery for different time periods allows for the assessment of temporal changes in the turbidity of surficial water bodies, thereby providing a useful monitoring and management tool. Although remote sensing has proven to be useful for estimating turbidity, only a few studies have been devoted to quantifying the turbidity of rivers impacted by mine tailings using this tool (e.g., Rudorff et al. 2018). To fill this gap, this study aimed to develop a framework for monitoring the spatiotemporal variation of turbidity in rivers that have been impacted by mine tailing discharge, by producing a model to predict turbidity based on Sentinel-2 imagery, using the Paraopeba River as a case study.

MATERIALS AND METHODS

Study area characterization

The study area is located in south-central Minas Gerais, Brazil, which is the largest producer of iron ore in the country. Possessing a diverse geological makeup, the region has experienced mining activity since the Brazilian colonial period. The hydrographic basin of the Paraopeba River, one of the main tributaries of the São Francisco River, has a length of approximately 510 km, covers 13,643 km², and

includes 35 municipalities. The Paraopeba River's source is located in the southern portion of the municipality of Cristiano Otoni, and its mouth is located in the Três Marias Reservoir in the municipality of Felixlândia.

On January 25, 2019, an abrupt failure of a mine tailing dam released 12 million cubic meters of mine tailings, most of which was discharged into the Paraopeba River. Immediately after the dam failure and discharge of the tailings, turbidity values increased to three or four orders of magnitude greater than those naturally observed in the river, with measurements in January exceeding 50,000 NTU (CPRM 2019). Owing to the abundant iron oxides in the mine tailings, the resulting turbidity plumes ranged in color from reddish to brownish (Teramoto et al. 2020).

To evaluate the impacts on turbidity associated with the entry of tailings into the Paraopeba River, natural turbidity variations must also be considered. Thus, we characterized the natural variability of the Paraopeba River turbidity, for the period preceding the rupture of the dam, using measured turbidity data for 2012 to 2018, collected by the Minas Gerais Water Management Institute (IGAM 2018) and the National Water Agency (ANA). Periodic monitoring information is available on the IGAM website.

Acquisition and processing of Sentinel-2 images

Our analysis was carried out using imagery from Sentinel-2, a multispectral satellite from the Copernicus Programme (European Space Agency 2022). The Sentinel-2 mission is composed of a constellation with two twin satellites (Sentinel-2A and Sentinel-2B) that systematically acquires spectral imagery from the Earth's surface. The set of Sentinel-2 bands, their central wavelengths, and spatial resolutions are listed in Table I.

We downloaded cloudless imagery to examine the spectral response of the Paraopeba River to spatiotemporal changes in turbidity. The Sentinel-2 satellite belongs to the Global

Table I. List of bands, central wavelengths, and spatial resolution of Sentinel-2 imagery.

Sentinel-2 bands	Central Wavelength (nm)	Spatial resolution (m)
Band 1 – Coastal aerosol	442.7	60
Band 2 - Blue	492.4	10
Band 3 - Green	559.8	10
Band 4 – Red	664.6	10
Band 5 – Vegetation red edge	704.1	20
Band 6 – Vegetation red edge	740.5	20
Band 7 – Vegetation red edge	782.8	20
Band 8 -NIR	832.8	10
Band 8A – Vegetation red edge	864.7	20
Band 9 – Water vapor	945.1	60
Band 10 – SWIR - Cirrus	1373.5	60
Band 11 - SWIR	1613.7	20
Band 12 - SWIR	2202.4	20

Monitoring Program for Environment and Security (GMES) and is administered by the European Community and European Space Agency (ESA). In this study, the analysis was performed using images from the 29SQA tile (Sentinel-2 mission grid system). The downloaded images at Level-1C provide top-of-atmosphere (TOA) and reflectance atmosphere values after radiometric and geometric corrections are applied. Because the raw data are presented in the form of digital numbers (DN), the values must first be converted to physical units of reflectance by dividing by a rescaling factor known as the quantification value, according to Equation 1. The quantification value (Qv) is presented in the metafiles accompanying the Sentinel-2 imagery.

$$Reflectance = DN/Qv \quad (1)$$

Subsequently, the original images containing TOA reflectance at Level 1C were corrected to the bottom-of-atmosphere (BOA) using the Sen2Cor (version 2.8) processor, developed by Telespazio VEGA Deutschland GmbH on behalf of ESA, and were used for image processing (Malenovský et al. 2012). The conversion of TOA at level 1C to BOA at level 2A involved atmospheric, terrain, and cirrus corrections. Sen2Cor is based on a set of 24 lookup tables (LUTs) that cover most terrestrial atmospheric conditions and recreate values to generate an image through atmospheric correction processing. We used Sen2Cor as a plugin integrated into the Sentinel Application Platform software (SNAP), which is freely distributed by the ESA.

In situ turbidity monitoring

The data for the nephelometric *in situ* turbidity of the Paraopeba River were measured daily at 49 stations, where 87 measurements were performed (Figure 1) using a manual turbidimeter at different times. These sample points were distributed downstream from the site of dam failure, along approximately 300 km of the watercourse between the dam and its entry into the Três Marias Reservoir.

Determination of an empirical model for turbidity estimates

Based on the results presented by Chen et al. (2007), Nechad et al. (2010), Dogliotti et al. (2015), Caballero et al. (2019), Rudorff et al. (2018), and Sakuno et al. (2018), we hypothesized that turbidity values could be obtained by using empirical models based on a single band. Hence, this study seeks to develop a representative empirical model. Reflectance values were extracted from Sentinel-2 images at the *in situ* turbidity measurement points and compared to the field-measured turbidity values.

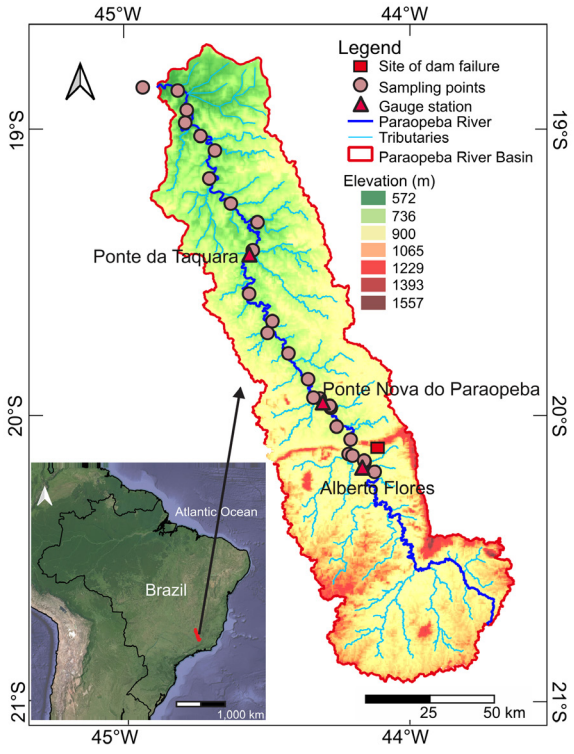

Figure 1. Location of the study area and distribution of the 49 *in situ* turbidity monitoring stations; site of the dam failure, and three gauge stations.

From the construction of a scatter plot of the turbidity values versus the reflectance data of the Sentinel-2 bands 2 to 8A, non-linear regression analysis was performed to identify the band most capable of reproducing the turbidity variations *in situ*. To measure the accuracy of values predicted by non-linear regression, we evaluated the error, defined as the difference between the observed and estimated values of turbidity. The main statistical parameter to determine was the standard error regression (S) (Equation 2), which describes the average distance between the observed values from the fitted model:

$$S=\sqrt{\frac{1}{n-2}\left[T_{obs}-T_{est}\right]^2} \quad (2)$$

where n denotes the number of samples, and T_{obs} and T_{est} represent the observed and estimated turbidity values, respectively.

Among the tested Sentinel-2 bands, those that offered the lowest S were evaluated, considering these as the most representative bands for use in obtaining turbidity estimates. Consequently, the equations derived from the regression analysis with the lowest S values were considered the most appropriate for estimating the turbidity of the Paraopeba River from Sentinel-2 images.

RESULTS

Turbidity preceding failure of the mine tailing dam

Generally, turbidity exhibits seasonal and cyclical behavior according to the precipitation volume. Therefore, the data compiled for turbidity between 2012 and 2018 were grouped into rainy (between October and March) and dry periods (between April and September).

Figure 2 presents a box diagram comparing turbidity in the rainy and dry seasons; the average turbidity in the rainy season (88.13 NTU) was significantly higher than that in the dry season (20.56 NTU). We also noted the presence of outliers, with values above 500 NTU, particularly during the rainy season. Only three samples showed turbidity values above 1,000 NTU, revealing that extremely high turbidity was very unusual before mine tailing introgression into the Paraopeba River.

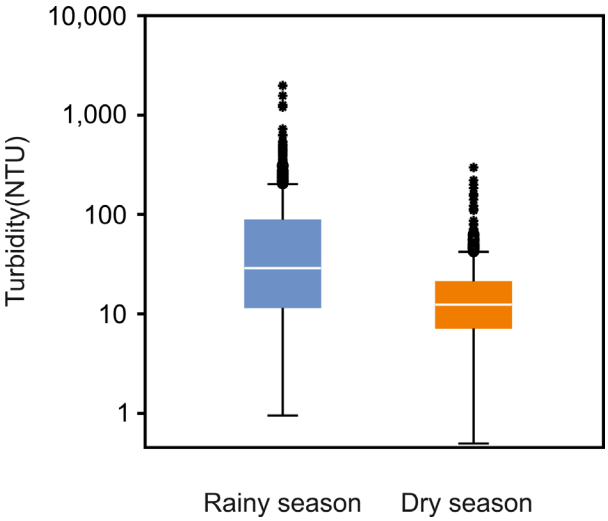

Figure 2. Box diagram for turbidity values in the rainy (October to March) and dry (April to September) periods between 2012 and 2018. The turbidity values are presented on a logarithmic scale. The central line inside the box represents the median, and the upper and lower limits of the box represent the first and third quartiles values, respectively. The distinctiveness of turbidity during dry and wet seasons is controlled by the variation of the river flow.

Turbidity monitoring after failure of the mine tailing dam

As shown in Figure 2, there is a noticeable difference between turbidity in the dry and wet seasons before the Brumadinho Dam failure, suggesting a direct association between the seasons and the river flow, with turbidity increasing as the flow increased. To evaluate the variation in turbidity after dam failure as a response to seasonal variations in river flow, we built hydrographs with data from three gauge

stations during 2019 (Figure 3), the locations of which are shown in Figure 1. As shown in Figure 3, the river flow at all gauge stations was higher between January and April, then strongly decreased after April, and abruptly increased at the end of September, with a discharge magnitude similar to that observed during February and March.

The monitoring results from January to December 2019 are presented as boxplot diagrams in Figure 4. Notably, the recorded values in the 2019 dry season were substantially higher than those observed in the dry periods before the dam failure (Figure 2).

In addition, the temporal variation in turbidity strongly matches the variation in river flow (Figure 3), showing evidence of the direct dependence of turbidity on river discharge. Similar to the river flow, the turbidity experienced a progressive increase in median values, peaking in March and decreasing in the subsequent months. The lowest recorded turbidity was observed in August and September, the driest periods of the year. During the beginning of the wet season in September, the median of turbidity values increased significantly, reaching values closer to those observed during February and March.

The movement of the turbidity plume was mediated by the advective movement within the Paraopeba River flux and reached the Retiro Baixo Reservoir, located nearly 270 km downstream of the dam failure site, two months later. Figure 5 shows the true color composition of the Retiro Baixo Reservoir during the three different periods as follows: The first image (Figure 5a), from January 22, 2019, three days before the rupture of Dam I, shows reduced values of water turbidity. Figure 5b shows the arrival of the turbidity plume at the Retiro

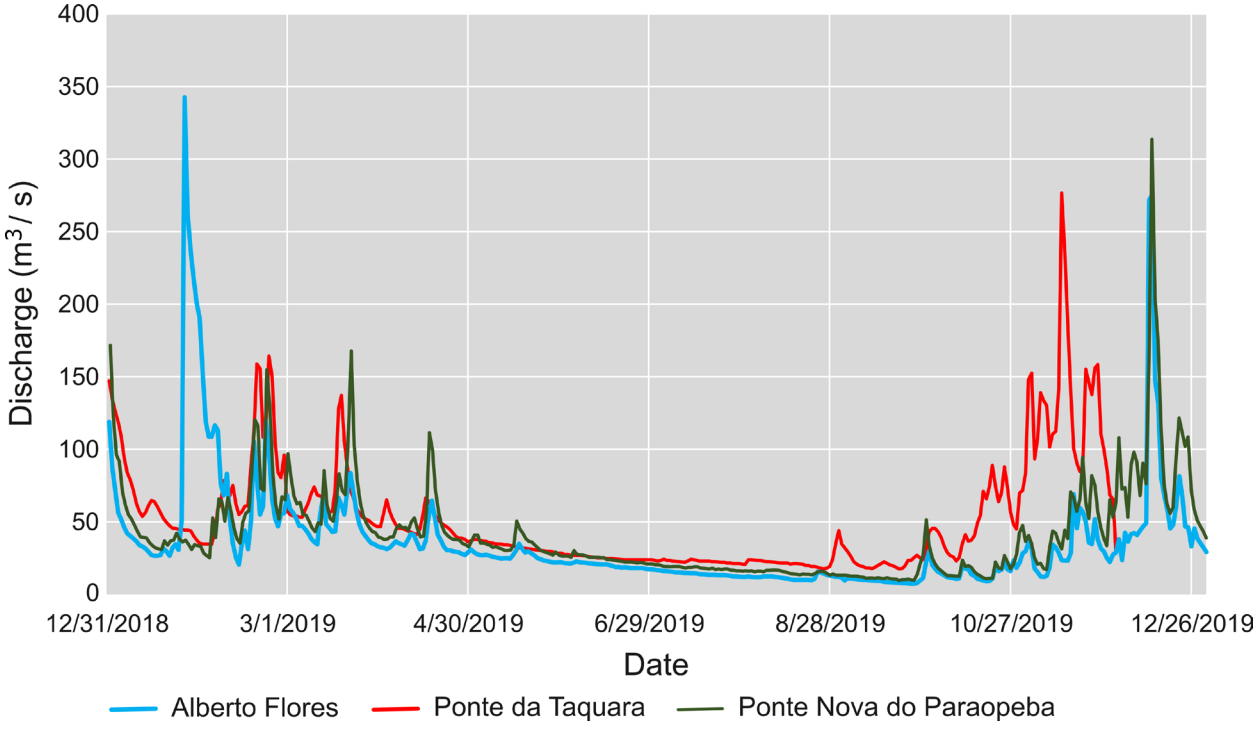

Figure 3. Hydrographs from the three gauge stations observed during 2019 (locations are shown in Figure 1). The highest discharge values were recorded between January and April, falling afterward and then increasing at the end of September in response to the variation of rainfall.

Baixo Reservoir on March 8, 2019, when the turbidity values increased significantly. Figure 5c shows the turbidity on May 27, 2019, when the turbidity had attenuated to some degree.

Regression of reflectance values and spatial resolution

The measurement of in situ turbidity values and the recording of Sentinel-2 scenes were performed on the same days, allowing for direct comparison between the turbidity and reflectance values at the different sampling points.

Non-linear regression analysis revealed that an exponential model provided the best fit of the spectral response data and 87 in situ measured values of turbidity. To identify the individual Sentinel-2 bands that offered the best estimation of turbidity, we evaluated the values of the fitted exponential R^2 model for each band. We found that the red edge of the vegetation (band 7) and NIR band (band 8) provided the highest R^2 values. We preferred to use band 8 because it has a spatial resolution of 10 m, which is more appropriate for the dimensions of the Paraopeba River, which has a width ranging between 25 and 70 m. Figure 6 shows the scatterplot of turbidity values with the reflectance of band 8 with the exponential equation, with an R^2 of 0.91. We used the resulting non-linear equation, to produce turbidity estimates from Band 8, as shown in Equation 3.

$$Turbidity = 3.535 * e^{39.324 * pw} \quad (3)$$

As shown in Figure 6, the deviation of the observations from the model curve is higher for turbidity above 300 NTU. Because the field-measured turbidity encompasses three orders of magnitude, S (381.05 NTU) reflects the errors of the highest values. Thus, we computed S for distinct turbidity ranges to evaluate the effective representation of the produced model. Figure 7 illustrates the comparison of S with distinct values of field-measured turbidity, showing that S increased as the turbidity increased.

Time-series of turbidity derived from the empirical model

To assess the consistency of the proposed empirical model, distribution maps of turbidity

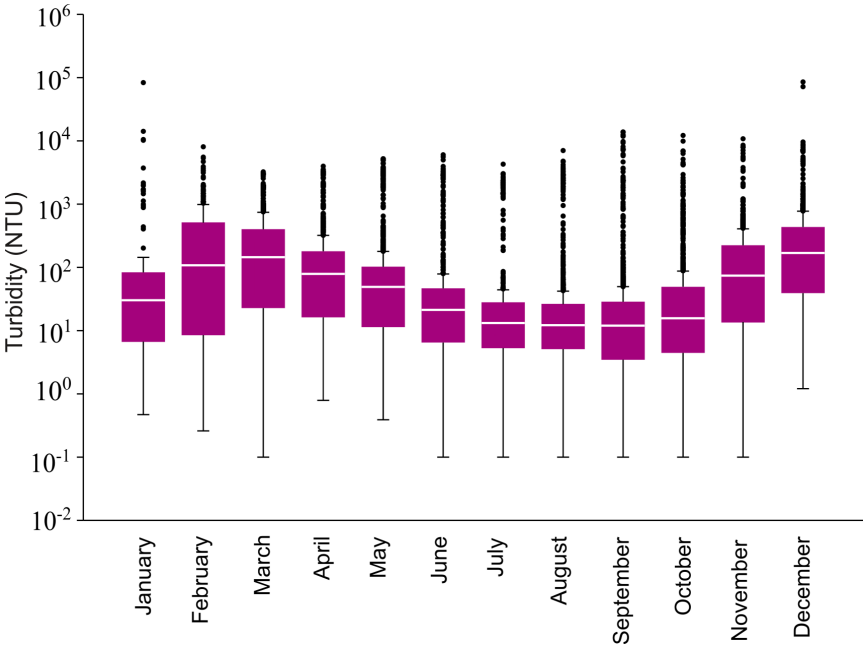

Figure 4. Variations in turbidity values between January and December 2019. The central line inside the box represents the median, and the upper and lower limits of the box represent the first and third quartiles values, respectively. The turbidity follows a seasonal variation, in which the highest values are observed during the rainy season in February and March, steadily decreasing afterward and then increasing at the end of September, strongly matching the variation of river flow shown in Figure 3.

estimated from the application of Equation 3 to imagery retrieved from the Sentinel-2 satellite, were produced for the periods before and after the dam rupture (Figure 8).

The estimated turbidity distribution for January 22, 2019 (Figure 8a), three days before the dam failure, showed values below 100 NTU. Conversely, on March 8, 2019 (Figure 8b), 42 days after the dam failure, remarkably high values of turbidity were estimated, reaching above 500 NTU and demonstrating the transport of a large amount of suspended material. The turbidity estimated on May 27, 2019 (Figure 8c), 122 days after the dam failure, showed a reduction in turbidity compared to that of March. In September 2019, the turbidity reached its lowest value at the end of the dry season (Figure 8d) because of the reduced river flow observed during this period.

DISCUSSION

The Paraopeba River is one of the main tributaries of the São Francisco River and an important source of water supply and irrigation for several municipalities in the central region of the state of Minas Gerais. The failure of the dam on the Paraopeba River resulted in environmental and social devastation; however, the true magnitude of long-term impacts resulting from the input of mining waste remains unclear. In this context, the importance of monitoring water quality is

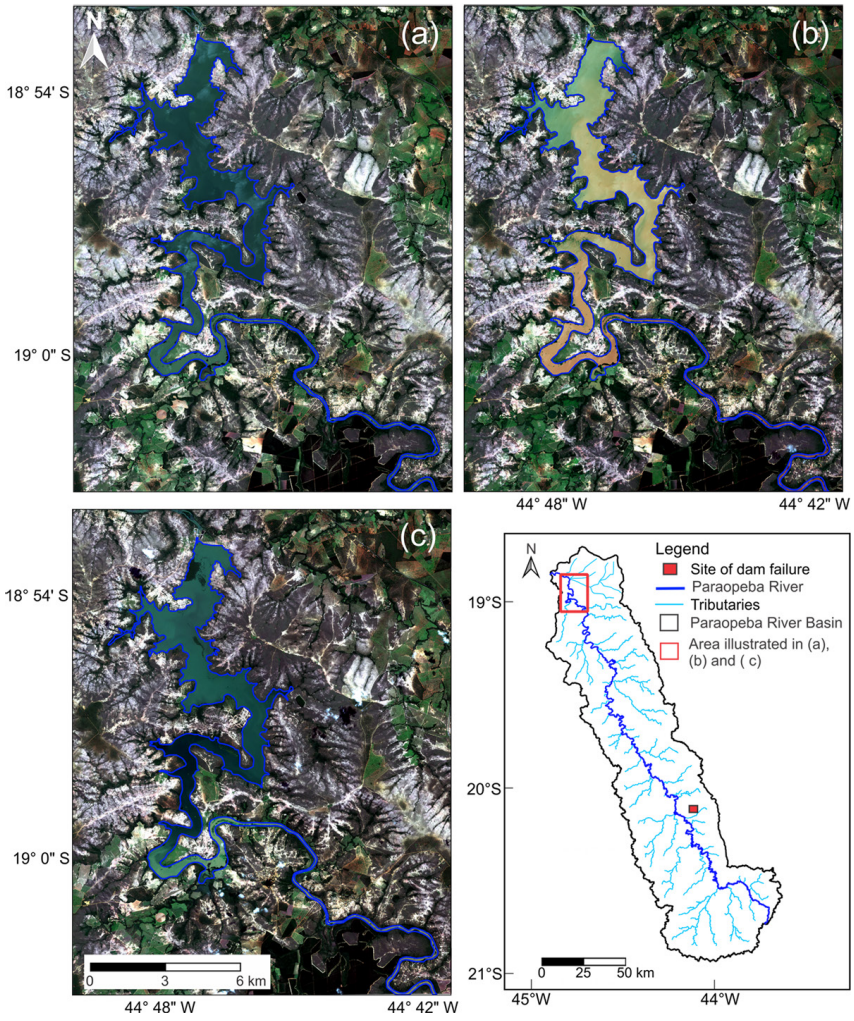

Figure 5. True color composition by red-green-blue for three different dates and representative periods: a) January 22, 2019, three days before the rupture of the mine tailing dam, when the turbidity values were relatively low; b) March 8, 2019, 42 days after the rupture of the mine tailing dam, when the turbidity plume reached the dam; and c) May 27, 2019, 122 days after the rupture of the mine tailing dam, when a large proportion of the turbidity plume had dissipated. The turbidity plumes in (a) and (b) are easily recognized by regions of brownish color, reflecting the nature of the mine tailings, which are rich in iron-oxides.

highlighted in the assessment of the long-term negative impacts of the introduction of mine tailings into the rivers.

The strong increase in turbidity values represents the main environmental impact associated with the tailing dam failure, making the river water unfit for human consumption. Consequently, the development of techniques for monitoring turbidity has high social and environmental relevance.

The results presented in this study indicate that, considering the local physical characteristics of the river system (i.e., width of the water body and nature of the suspended materials), the NIR band 8 of the Sentinel-2 satellite offers the best fit to the measured turbidity, allowing for the monitoring of turbidity variation over time at the regional scale. Owing to the average temporal revisit-frequency solution of five days, Sentinel-2 allows for the construction of a detailed historical series. For this reason, the systematic monitoring of turbidity variations in the Paraopeba River can be conducted using remote sensing techniques.

Importantly, the estimation of river turbidity by remote sensing shown here and in previous studies (e.g., Petus et al. 2010, Pereira et al. 2018, Kuhn et al. 2019) does not have the same accuracy as measurements performed in the field. The estimation of turbidity using remote sensing has a distinct purpose compared to field measurements. While field measurement still represents the best method for the quantitative assessment of turbidity, it offers only single-point values. Alternatively, the approach sensing offers the possibility of more continuous monitoring of the river, allowing the identification of spatial and temporal trends throughout the entire stream. Another attractive advantage of turbidity monitoring using remote sensing is the relatively low cost of obtaining data and estimating values for the full course of the river.

Although remote sensing techniques have been demonstrated in previous studies on coastal regions (e.g., Nechad et al. 2010, Petus et al. 2010, Dogliotti et al. 2015) and lakes (Sakuno et al. 2010), few studies have demonstrated the use of remote sensing to monitor turbidity in rivers. This study identified a model that allows for consistent turbidity estimates from Sentinel-2 imagery of the Paraopeba River. Importantly, owing to the specificity with respect to the type and characteristics of the suspended material, the empirical model relating turbidity to the spectral response of the satellite imagery

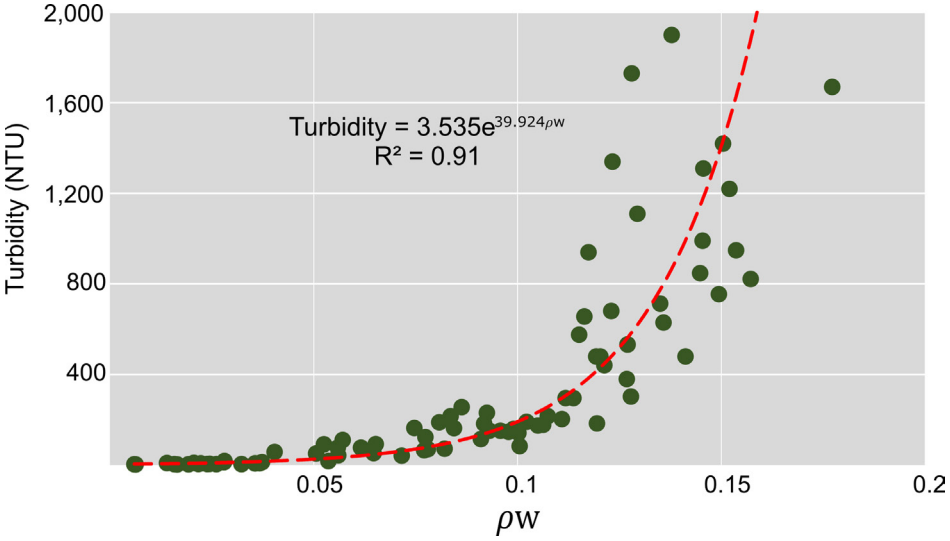

Figure 6. Dispersion graph of the reflectance from one infrared band of Sentinel-2 (band 8) and turbidity values (green points) with the exponential model (red line). The deviation of the observed values from the model curve increases as the turbidity increases.

is site-specific. Similarly, the models developed for the other sites could not be used in our case.

Although there is a large diversity of models to produce reliable estimates of turbidity based on the spectral response of satellite imagery, some are based on a single-band model, which is a simplistic approach that correlates turbidity with the variation of reflectance at a particular wavelength (e.g., Dogliotti et al. 2015, Guo et al. 2017, Caballero et al. 2019). Despite its simplicity, our work demonstrates that in the case of river water impacted by mine tailings, the single-model approach produces reliable turbidity estimates. Importantly, the temporal evolution of turbidity estimated by our model (Figure 7) closely resembled that measured in the field (Figure 4), in which the highest values were observed in February and March, then decreased in consecutive months and reached the lowest values in September, at the end of the dry season. Thus, our model can produce a reliable time series of turbidity and can be used as a complementary tool to estimate the spatiotemporal behavior of this parameter. Despite the ability of our empirical model to produce consistent estimates of turbidity, this model is site-specific and serves to monitor the suspended material transported by the Paraopeba River, impacted by iron-rich tailings.

Regression analysis indicates that the exponential model best fits the turbidity data as a function of the spectral response of the analyzed band. This is justified by the fact that the turbidity presents variations of several orders of magnitude, whereas the reflectance varies linearly. Notably, the deviation of the observed turbidity from the fitted model increased as the turbidity increased (Figure 6), implying that the quantitative evaluation of extremely high turbidity is less reliable. The greater discrepancy associated with increasing turbidity might be a consequence of inaccuracies in the turbidimeter used in this turbidity range, or it may be that the spectral response saturates at higher turbidity levels. Because the turbidity encompasses values varying by several orders of magnitude,

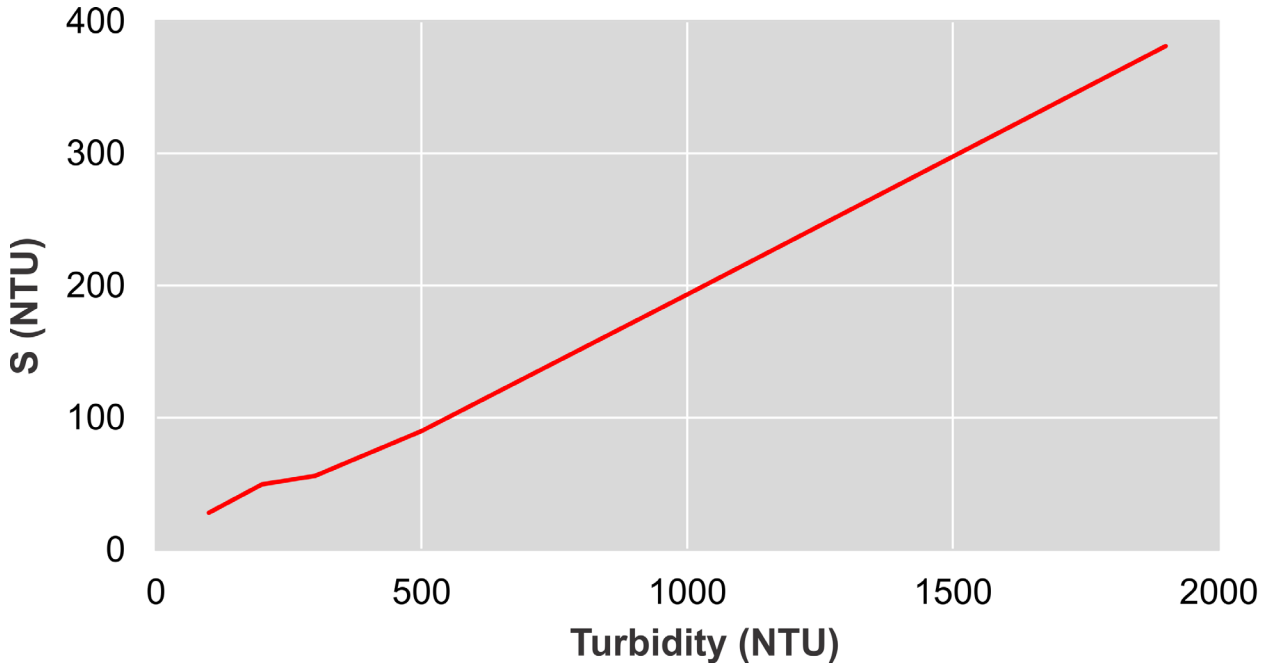

Figure 7. Computed values of S as function of field measured turbidity, showing that the error linearly increases as the turbidity increases.

the obtained S (381.05 NTU) is essentially controlled by the elevated error measured at high values. The error was reduced when intervals with smaller values were considered. For example, if turbidity values of 50 NTU are considered, the computed error will be 5.26 NTU, demonstrating that the quantitative assessment of extremely high values of turbidity is limited.

Despite the absence of the same level of accuracy found in field measurements, the use of an approach based on the remote sensing can produce reliable and consistent estimates of turbidity. To demonstrate the practical application of our model, we built a time series of turbidity calculated by our empirical model (Figure 6), which followed a similar trend to that observed in the field measurements (Figure 4).

The actual extent of metal contamination of the Paraopeba River induced by mine tailing input remains controversial. Some studies have demonstrated the intense impact of dissolved metals in the river water (Santos Vergilio et al. 2020, Thompson et al. 2020), whereas others have argued that the physical and chemical characteristics of the river cannot maintain high concentrations of metals in dissolved form (Teramoto et al. 2020). Teramoto et al. (2020) verified an increase in metals during the rainy season, which was related to an increase in suspended sediments. Consequently, the severe increase in the movement of the turbidity plume may represent the main mechanism controlling the metal transport in river water. This scenario is consistent with some studies that associate metal transport with turbidity (e.g., Swain & Sahoo 2017, Nasrabadi et al. 2016).

The behavior of mine tailings in the Paraopeba River may represent a seasonal phenomenon, in which resuspension is expected to occur along with an increase in river flow. However, during the dry season, because the river flow tends to decrease significantly, the transported mine tailings are expected to be deposited in the riverbed. Thus, our model serves as a valuable tool for the long-term monitoring of river turbidity and is a consistent method to assess water quality.

The most important contribution of our work is to demonstrate the capability of to accurately estimating turbidity based on single-band models, with the NIR band identified as the most consistent band for predicting turbidity.

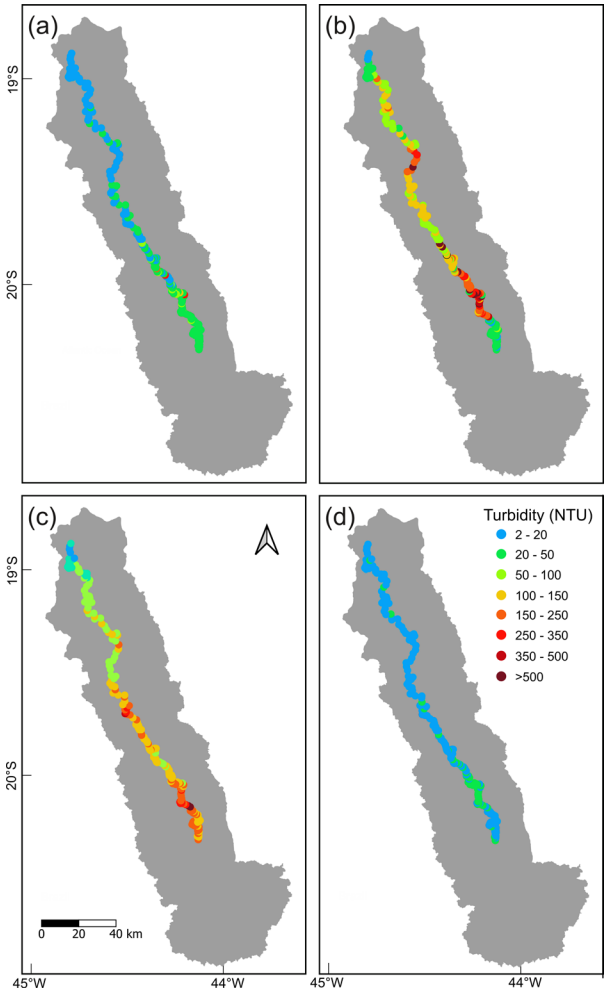

Figure 8. Estimated turbidity distribution map for 206 points distributed along the course of the Paraopeba River: a) January 22, 2019; b) March 8, 2019; c) May 27, 2019; and d) September 19, 2019. The highest turbidity was observed during March 2019, declining in the following months, and reaching lower values in September 2019. This trend strongly matches with the general trend seen in the field measurements, shown in Figure 4.

Our approach has the advantage of being able to estimate turbidity at a lower cost than in situ measurements and can be applied using freely distributed satellite images. Consequently, this approach could allow environmental agencies, academic institutions, and society in general, to monitor the long-term adverse effects of mining activities on surficial watercourses, which are important sources of water supplies in many regions of the world.

CONCLUSIONS

The relatively large impact of mine tailing dam failure on the water quality of the Paraopeba River remains a source of concern. Although the long-term dynamics of discharged mine tailings remain unknown, water quality monitoring is a crucial issue. Among the recognized negative effects of the introgression of mine tailings, an increase in turbidity is the most important. Because turbidity represents an optical property, it can be inferred from the spectral response of satellite imagery. As a strategy to monitor the seasonal variation of turbidity, we matched 87 measured turbidity values with spectral responses of Sentinel-2 satellite data and produced an exponential model that successfully predicted the spatial distribution of turbidity in surficial water bodies, using the spectral response of the NIR band 8 (λ = 865 nm), with an R^2 of 0.91. Thus, our work reinforces the ability of the remote sensing approach to monitor the properties of surficial water bodies, and the single-band approach allows the attainment of strongly representative models, despite the simplicity of the approach. However, models predicting turbidity from spectral responses are site-specific, and the model obtained in this study is not capable of producing consistent predictions for other sites with different compositions and characteristics of suspended materials. We found that the deviation of field data from model predictions increased as the turbidity increased, but closely matched the most common range of in situ measured turbidity. Importantly, our model allows for a low-cost and simple strategy for monitoring turbidity and evaluating the long-term dynamics of discharged mine tailings over time along the course of the Paraopeba River.

Acknowledgments

The authors would like to thank the company Vale do Rio Doce S.A. for providing the turbidity data measured in situ. In addition, the authors thank FUNDUNESP for granting research grants.

REFERENCES

BILOTTA GS & BRAZIER RE. 2008. Understanding the influence of suspended solids on water quality and aquatic biota. Water Res 42(12): 2849-2861. https://doi.org/10.1016/j.watres.2008.03.018.

CABALLERO I, STUMPF RP & MEREDITH A. 2019. Preliminary assessment of turbidity and chlorophyll impact on bathymetry derived from Sentinel-2A and Sentinel-3A satellites in South Florida. Remote Sens 11(6): 645. https://doi.org/10.3390/rs11060645.

CHEN Z, HU C & MULLER-KARGER F. 2007. Monitoring turbidity in Tampa Bay using MODIS/Aqua 250-m imagery. Remote Sens Environ 109(2): 207-220. https://doi.org/10.1016/j.rse.2006.12.019.

CPRM - SERVIÇO GEOLÓGICO DO BRASIL. 2019. Ruptura da Barragem do Complexo do Feijão em Brumadinho – MG: Boletim de Monitoramento Compartilhado do Rio Paraopeba: Boletim de monitoramento compartilhado do rio Paraopeba, Belo Horizonte, 08 mar. 2019.

DAVIES-COLLEY RJ & SMITH DG. 2001. Turbidity suspended sediment, and water clarity: a review. J Am Water Resour Assoc 37(5): 1085-1101. https://doi.org/10.1111/j.1752-1688.2001.tb03624.x.

DOGLIOTTI AI, RUDDICK KG, NECHAD B, DOXARAN D & KNAEPS E. 2015. A single algorithm to retrieve turbidity from remotely-sensed data in all coastal and estuarine waters. Remote Sens Environ 156: 157-168. https://doi.org/10.1016/j.rse.2014.09.020.

EUROPEAN SPACE AGENCY. 2022. Sentinel-2. https://sentinel.esa.int/web/sentinel/missions/sentinel-2. Accesed 28 August 2022.

GÖRANSSON G, LARSON M & BENDZ D. 2013. Variation in turbidity with precipitation and flow in a regulated river system–river Göta Älv, SW Sweden. Hydrol Earth Syst Sci 17(7): 2529-2542. https://doi.org/10.5194/hess-17-2529-2013.

GUO K, ZOU T, JIANG D, TANG C & ZHANG H. 2017. Variability of Yellow River turbid plume detected with satellite remote sensing during water-sediment regulation. Cont Shelf Res 135: 74-85. https://doi.org/10.1016/j.csr.2017.01.017.

HAMILTON AK ET AL. 2020. Seasonal turbidity linked to physical dynamics in a deep lake following the catastrophic 2014 Mount Polley mine tailings spill. Water Resour Res 56(8): e2019WR025790. https://doi.org/10.1029/2019WR025790.

HENLEY WF, PATTERSON MA, NEVES RJ & LEMLY AD. 2000. Effects of sedimentation and turbidity on lotic food webs: a concise review for natural resource managers. Rev in Fisheries Sci 8(2): 125-139. https://doi.org/10.1080/10641260091129198.

HUANG WW, ZHANG J & ZHOU ZH. 1992. Particulate element inventory of the Huanghe (Yellow River): a large, high-turbidity river. Geochim Cosmochim Acta 56(10): 3669-3680. https://doi.org/10.1016/0016-7037(92)90160-K.

IGAM - INSTITUTO MINEIRO DE GESTÃO DE ÁGUAS. 2018. Monitoramento da Qualidade das Águas. http://www.igam.mg.gov.br/monitoramento-da-qualidade-das-aguas2. Accessed 12 November 2020.

KIRK JTO. 1985. Effects of suspensoids (turbidity) on penetration of solar radiation in aquatic ecosystems. Hydrobiologia 125(1): 195-208. https://doi.org/10.1007/BF00045935.

KUHN C. 2019. Performance of Landsat-8 and Sentinel-2 surface reflectance products for river remote sensing retrievals of chlorophyll-a and turbidity. Remote Sens Environ 224: 104-118. https://doi.org/10.1016/j.rse.2019.01.023.

MALENOVSKÝ Z, ROTT H, CIHLAR J, SCHAEPMAN ME, GARCÍA-SANTOS G, FERNANDES R & BERGER M. 2012. Sentinels for science: Potential of Sentinel-1,-2, and-3 missions for scientific observations of ocean, cryosphere, and land. Remote Sens Environ 120: 91-101. https://doi.org/10.1016/j.rse.2011.09.026.

NASRABADI T, RUEGNER H, SIRDARI ZZ, SCHWIENTEK M & GRATHWOHL P. 2016. Using total suspended solids (TSS) and turbidity as proxies for evaluation of metal transport in river water. Appl Geochem 69: 1-9. https://doi.org/10.1016/j.apgeochem.2016.03.003.

NECHAD B, RUDDICK KG & PARK Y. 2010. Calibration and validation of a generic multisensor algorithm for mapping of total suspended matter in turbid waters. Remote Sens Environ 114: 854-866. https://doi.org/10.1016/j.rse.2009.11.022.

PEREIRA LS, ANDES LC, COX AL & GHULAM A. 2018. Measuring Suspended-Sediment Concentration and Turbidity in the Middle Mississippi and Lower Missouri Rivers Using Landsat Data. J Am Water Resour Assoc 54(2): 440-450. https://doi.org/10.1111/1752-1688.12616.

PETTICREW EL. 2015. The impact of a catastrophic mine tailings impoundment spill into one of North America's largest fjord lakes: Quesnel Lake, British Columbia, Canada. Geophys Res Lett 42(9): 3347-3355. https://doi.org/10.1002/2015GL063345.

PETUS C, CHUST G, GOHIN F, DOXARAN D, FROIDEFOND JM & SAGARMINAGA Y. 2010. Estimating turbidity and total suspended matter in the Adour River plume (South Bay of Biscay) using MODIS 250-m imagery. Continental Shelf Res 30(5): 379-392. https://doi.org/10.1016/j.csr.2009.12.007.

POLIGNANO MV & LEMOS RS. 2020. Rompimento da barragem da Vale em Brumadinho: impactos socioambientais na Bacia do Rio Paraopeba. Cienc Cult 72(2): 37-43. http://dx.doi.org/10.21800/2317-66602020000200011.

RUDORFF N, RUDORFF CM, KAMPEL M & ORTIZ G. 2018. Remote sensing monitoring of the impact of a major mining wastewater disaster on the turbidity of the Doce River plume off the eastern Brazilian coast. ISPRS J Photogramm Remote Sens 145: 349-361. https://doi.org/10.1016/j.isprsjprs.2018.02.013.

SAKUNO Y, YAJIMA H, YOSHIOKA Y, SUGAHAR S, ABD ELBASIT MA, ADAM E & CHIRIMA JG. 2018. Evaluation of unified algorithms for remote sensing of chlorophyll-a and turbidity in Lake Shinji and Lake Nakaumi of Japan and the Vaal Dam Reservoir of South Africa under eutrophic and ultra-turbid conditions. Water 10(5): 618. https://doi.org/10.3390/w10050618.

SANTOS VERGILIO C ET AL. 2020. Metal concentrations and biological effects from one of the largest mining disasters in the world (Brumadinho, Minas Gerais, Brazil). Sci Rep 10(1): 1-12. https://doi.org/10.1038/s41598-020-62700-w.

SWAIN R & SAHOO B. 2017. Mapping of heavy meal pollution in river water at daily time-scale using spatio-temporal fusion of MODIS-aqua and Landsat satellite imageries. J

Environmental Manag 192: 1-14. https://doi.org/10.1016/j.jenvman.2017.01.034.

TERAMOTO EH, GEMEINER H, ZANATTA MB, MENEGÁRIO AA & CHANG HK. 2020. Metal speciation of the Paraopeba river after the Brumadinho dam failure. Sci Total Environ 757: 143917. https://doi.org/10.1016/j.scitotenv.2020.143917.

THOMAS S, RIDD PV & DAY G. 2003. Turbidity regimes over fringing coral reefs near a mining site at Lihir Island, Papua New Guinea. Mar Pollut Bull 46(8): 1006-1014. https://doi.org/10.1016/S0025-326X(03)00122-X.

THOMPSON F ET AL. 2020. Severe impacts of the Brumadinho dam failure (Minas Gerais, Brazil) on the water quality of the Paraopeba River. Sci Total Environ 705: 135914. https://doi.org/10.1016/j.scitotenv.2019.135914.

WASS PD, MARKS SD, FINCH JW, LEEK GJXL & INGRAM JK. 1997. Monitoring and preliminary interpretation of in-river turbidity and remote sensed imagery for suspended sediment transport studies in the Humber catchment. Sci Total Environ 194: 263-283. https://doi.org/10.1016/S0048-9697(96)05370-3.

WHO - WORLD HEALTH ORGANIZATION. 2017. Guidelines for drinking-water quality. https://apps.who.int/iris/rest/bitstreams/1080656/retrieve. Accessed 12 November 2020.

How to cite

CRIONI PLB, TERAMOTO EH & CHANG HK. 2023. Monitoring river turbidity after a mine tailing dam failure using an empirical model derived from Sentinel-2 imagery. An Acad Bras Cienc 95: e20220177. DOI: 10.1590/0001-3765202320220177.

Manuscript received on February 22, 2022;
accepted for publication on August 25, 2022

PEDRO L.B. CRIONI[1]
https://orcid.org/0000-0003-1500-738X

ELIAS H. TERAMOTO[1,2]
https://orcid.org/0000-0002-3072-6801

HUNG K. CHANG[1,2,3]
https://orcid.org/ 0000-0002-6274-4510

[1]Universidade Estadual de São Paulo (UNESP), Laboratório de Estudos de Bacias (LEBAC), Avenida 24A, 1515, Bela Vista, 16506-900 Rio Claro, SP, Brazil

[2]Universidade Estadual de São Paulo (UNESP), Centro de Estudos Ambientais, Avenida 24A, 1515, Bela Vista, 16506-900 Rio Claro, SP, Brazil

[3]Universidade Estadual de São Paulo (UNESP), Departamento de Geologia Aplicada, Avenida 24A, 1515, Bela Vista, 16506-900 Rio Claro, SP, Brazil

Correspondence to: **Pedro L.B. Crioni**
E-mail: pedro.crioni@unesp.br

Author contributions

P.L.B. Crioni and E.H. Teramoto contributed to the acquisition of data and the manipulation of the information obtained for the construction of the empirical model. H.K. Chang confirmed the results obtained and organized the manuscript for publicati on. All authors participated in the writing of the article.